Chemical Physics Letters 768 (2021) 138398

Contents lists available at ScienceDirect

Chemical Physics Letters

journal homepage: www.elsevier.com/locate/cplett

Research paper

Evaluating and understanding the affinity of metal ions to water and ammonia using density functional theory calculation

Xue-Yun Shang [a,b], Hua-Ying An [b], Ting Zhang [b], Jin-Hong Lin [b], Fei Hao [a,*], Dong-Hai Yu [b,*], Ji-Chang Xiao [b,*], Tian-Duo Li [a,*]

[a] Shandong Key Laboratory of Molecular Engineering, School of Chemistry and Chemical Engineering, Qilu University of Technology (Shandong Academy of Sciences), Jinan 250353, China

[b] Key Laboratory of Organofluorine Chemistry, Shanghai Institute of Organic Chemistry, University of Chinese Academy of Sciences, Chinese Academy of Sciences, Shanghai 200032, China

ARTICLE INFO

Keywords:
Metal ion affinity
Ligand exchange model
Energy decomposition analysis
Natural bond orbital analysis
Information-theoretic approach in density functional reactivity theory

ABSTRACT

Affinity, which is the essential attribute of metal ions, is very important to their physical and chemical properties. To make quantitative description and deep understanding on the affinity, fourteen metal ions were considered, and two representative ligands (H_2O and NH_3) were selected. Five types of energy of five models have been calculated using the density functional theory. Then, the results have been applied to quantify the affinity and describe its evolution in the ligand exchange process. Three aspects, energy decomposition analysis, natural bond orbital analysis, and information-theoretic approach in density functional reactivity theory, have been considered to understand the affinity.

1. Introduction

The affinity of metal ion to ligand plays an important role in various fields, such as chemistry, biology, industry, even whole nature [1–3], and has a great influence on various properties of metal ions, such as dissolution [4], catalysis [3], migration [1], coordination [5], biocompatibility [2,6], recognition [2], etc.. Therefore, many efforts have been paid on it. The binding energy between ligands and metal ions is a valid criterion used to directly evaluate the affinity [6]. For instance, the hydration energy of beryllium and magnesium ions was investigated with ab Initio methods by Markham et al., which concluded that the long-range interaction, namely the outer hydration shell, should be considered to calculate the affinity with water [7]. The geometrical and energetical features of hydration complexes of several 3d ions from Sc (III) to Fe(III) have been calculated by Kallies et al. using the density functional theory, which found that the charge-transfer contribution analyzed from natural bond orbital is similar to that obtained from classical ligand field theory [8]. One of the widest applications of the affinity of metal ions is the ion chromatography, which is the indispensable instrument in chemical laboratory [1]. Moreover, there are many other literatures relating to the affinity [9,10].

Comparing to the absolute affinity (i.e., the bonding energy), the relative affinity (i.e., the ligand exchange energy) between different metal ions and ligands (which belonging to same series) is more convenient to predict the thermodynamically favorable bonding [10], ionic separation [1], ionic recognition [2], etc.. The ligand-exchange model is a widely used approach to investigate the relative affinity of metal ions to different ligands and other related properties. For example, Varadwaj et al. found that the Ni(II) and Co(II) complexes would add stability of 7 ± 2 and 6 ± 1 kcal/mol respectively if per H_2O was replaced by NH_3 [11,12]. Namely, both of the Ni(II) and Co(II) have stronger affinity to NH_3 than H_2O, although the magnitude of affinity is different. The similar approach was also applied on the bonding energies of complexes of Mn(II), Co(II), Ni(II), Cu(II), and Zn(II) with H_2O and NO_3^- [13], the coordination state probabilities of Zn(II) in the mixture of H_2O and CH_3OH [14], the interaction between dipicolinic acid and hydrated Fe(II) [15], and the relative stability of Tb(III) with several substituted pyridinecarboxylic acids [16]. Then, Varadwaj et al also reported the calculated Irving-Williams thermodynamic series of several metal ions with some non-chelating ligands to predict the experimental sequence [17]. Nevertheless, Jover et al. calculated the binding affinities between monovalent cations (Li(I), Na(I), K(I), Cu(I), Ag(I)) and twenty common amino acids, which have been applied to search for the highest and lowest bonding [5].

* Corresponding authors.
E-mail addresses: fayehaofei@126.com (F. Hao), ydonghai@sioc.ac.cn (D.-H. Yu), jchxiao@sioc.ac.cn (J.-C. Xiao), litianduo@163.com (T.-D. Li).

https://doi.org/10.1016/j.cplett.2021.138398
Received 11 October 2020; Received in revised form 28 January 2021; Accepted 28 January 2021
Available online 1 February 2021

In most metal complexes, the coordination atoms are usually the nitrogen and/or the oxygen. To evaluate the affinity of metal ions to oxygen and/or nitrogen more reliably and understand more reasonably, numerous efforts have been paid from different perspectives, including experimental, theoretical and computational aspects [18]. In experimental aspects, besides the X-ray crystal diffraction, the X-ray absorption fine structure spectroscopy is also developed to directly determine the coordination structure of metal ion in solution [19], which result in the researcher can directly look the closest coordinated atoms. In theoretical aspects, the affinity has been described with different theories. For example, the famous hard and soft acids and bases (HSAB) principle is a qualitative guidance to describe the stability of complexes between metal ions and ligands, which is based on that the affinity is stronger between hard ion and hard ligand or soft ion and soft ligand, but it is weaker between hard ion and soft ligand or soft ion and hard ligand [18]. And the molecular orbital theory can be used to explain the affinity between metal ion and ligand [7]. In computational aspects, lots of methods, especial the density functional theory (DFT) have been widely applied to calculate the affinity of metal ion and ligand based on the geometry, energy, electron number, etc. [12,13,17,20]. In these three aspects, the computational approach is the most convenient, and gradually become the popular approach to explore the affinity of metal ion to ligands [7,11–13,17,20].

At initial, fourteen common metal ions (Na(I), Mg(II), Al(III), Ca(II), Sc(III), Ti(IV), V(II), Cr(II), Mn(II), Fe(III), Co(II), Ni(II), Cu(II), Zn(II), the most stable valence state has been chosen for each element), have been considered, because they are widely concomitant in various systems and they can be used to extend the evolution of affinity observed by Varadwaj et al. [11–13,17,20] to a wider range. And, NH_3 and H_2O were selected as the representative nitrogenous and oxygenic ligands respectively. In this work, the difference of energy calculated from different models are applied to quantify the relative affinity between different metal ions and ligands and to explore the evolution in ligand exchange process. Then, three approaches, energy decomposition analysis [21,22], natural bond orbital analysis [23] and information-theoretic approach in density functional reactivity theory [24], have been applied to understand the affinity.

2. Computational details

2.1. Model

For quantify the affinity of metal ion to ligand and evaluating its evolution in the ligand exchange process, five reaction equations listed in Table 1 are considered as the models, and the difference of energies of these reaction equations are calculated as the descriptors. The model A is idealized, the bare metal and unimolecular NH_3 and H_2O are used [11,12], this model is not the real process due to the hydration of charged metal ions and aggregation of NH_3 and H_2O, but it has been widely used to represent the reactions between the metal ions with NH_3 and H_2O. The model A is related to the bare metal ions, its reaction energy is a measurement of absolute affinity [8]. The model B, C and D are equivalent in mathematics, these three models can interconvert with other reaction equations of independent on the metal ions. But model B considers the protonation of NH_3 at acidic condition, and the aggregation of NH_3 and H_2O was considered in model D. According to the reports of Lee et al. and Nakai et al., the 4 and 5 could be regarded as a favorable aggregation number of water and ammonia molecules respectively [25,26], then adopted here. The model E is a new one, proposed here first time. In this model, for each complex, $[M(H_2O)_{6-n}(NH_3)_n]^{x+}$, the corresponding cage, $(H_2O)_{6-n}(NH_3)_n$, is applied as a reactant to calculate the reaction energies. The reason is that the NH_3 and H_2O in bulk phase are must different to them in the complexes, and they are also different in different coordination condition, at least they have different activity [27]. The model E can exclude the reorganization energies of H_2O and NH_3, this part energy could be regulated by the solvent molecules, but little affect to the coordination between metal ion and ligand. The model E could also eliminate the translational entropy effect caused by difference of molecular number on the two sides of reaction equation. Therefore, the calculated magnitude of reaction energy of model E could more purely reflect the affinity between metal ions and ligands. Moreover, a special cage of $(H_2O)_{6-n}(NH_3)_n$ is used for each complex in model E, and the model E is also be called cage exchange model.

Table 1
Five reaction equations applied to evaluate the affinity between metal ions and ligands. The metal ion is represented with Ni(II), and united with kJ/mol.

Model	Reaction equations	Ref.
A	$Ni^{2+} + (6\text{-}n)H_2O + nNH_3 \rightarrow [Ni(H_2O)_{6-n}(NH_3)_n]^{2+}$	[11,12]
B	$[Ni(H_2O)_6]^{2+} + nNH_4^+ \rightarrow [Ni(H_2O)_{6-n}(NH_3)_n]^{2+} + nH_3O^+$	[11]
C	$[Ni(H_2O)_6]^{2+} + nNH_3 \rightarrow [Ni(H_2O)_{6-n}(NH_3)_n]^{2+} + nH_2O$	[11,12]
D	$[Ni(H_2O)_6]^{2+} + n/5(NH_3)_5 \rightarrow [Ni(H_2O)_{6-n}(NH_3)_n]^{2+} + n/4(H_2O)_4$	[25,26]
E	$[Ni(H_2O)_6]^{2+} + (H_2O)_{6-n}(NH_3)_n \rightarrow [Ni(H_2O)_{6-n}(NH_3)_n]^{2+} + (H_2O)_6$	new

For all complexes, only the inner shell ligands, namely directly coordinated on the central metal ions are included, because of the outer shell ligands are interacting to the metal ions through the hydrogen bond with already coordinated ligand indirectly, and have little influence to the affinity of metal ions. For the complexes with six ligands, ten classical configurations have been considered, as Varadwaj et al.'s reports [11,12]. For each configuration, the structure with the lowest energy is selected to further analysis.

2.2. Theory

In density functional theory, the total energy could be decomposed to three components, noninteracting kinetic (T_S), electrostatic (E_e), and exchange-correlation (E_{XC}) energies [21,22]. These three components have been widely applied to explain the interaction between atoms [28], and also be used in current work. The natural bond orbital (NBO) analysis could decipher the molecular wavefunction to concepts commonly understood by chemists [23], such as Lewis structures, atomic charge, bond order, etc.. Here, several quantities from NBO analysis, the molecular electrostatic potential (MEP), atomic charge, and population of natural atom orbital (NAO) have been adopted. Three types of atomic charges, natural population analysis charge (NPA), electrostatic potential charge (ESP) and Hirshfeld charge (Hirshfeld) are used, and the population in three types of atomic valent orbital, s (NAO_s), p (NAO_p), (NAO_d), and their sum (NAO_all) are used. Additionally, the information-theoretic approach in density functional reactivity theory (ITA-DFRT) [24] developed recently is also used to understand the affinity from an unclassical perspective. The core idea of ITA-DFRT is that one can describe the reactivity of molecule using the ITA quantities directly calculated from electron density, and the essence of ITA quantities is the distribution characteristic of electron density. The ITA-DFRT have been successfully used to numerous aspects [24], including aromaticity/antiaromaticity [29], steric effect [30], electrophilicity/nucleophilicity [31], etc., but its availability in complexes is not clear up to now. Eight ITA quantities were calculated here, including Shannon entropy (S_S), a local functional of the electron density and a measure of the spatial delocalization of the electron density probably gained the most attention, Fisher information (I_F), a gauge of the sharpness or concentration of the electron density distribution, Ghosh-Berkowitz-Parr entropy (S_{GBP}), the local kinetic energy density and Thomas–Fermi kinetic energy density, information gain (I_G), a non-symmetric measure of the entropy difference between two probability distribution functions, second and third Onicescu information energy (E_2 and E_3), a finer measure of dispersion distribution than that of the Shannon entropy, and second and third relative Rényi entropy (${}^rR_2$ and ${}^rR_3$), a measure of the deviation of electron density from a reference

density [24].

2.3. Calculation

All calculations were performed at the DFT M06 [32]/6-311++G(d, p) [33] level of theory using the Gaussian 09 package version D01 [34] with the tight SCF convergence criterion and ultrafine integration grids. The tight option has been adopted to determine convergence of geometry optimization, and the default option has been used for frequency calculations. The single-point frequency calculation was performed based on the optimized structures to ensure that the final structure obtained has no imaginary frequency. Based on some test calculation about the metal ions that own more than one spin states (the results are collected in Table S4), the highest spin complexes have the lowest energy, then high spin state was adopted for the metal ions [11–13,20]. To exclude the reorganization energy of the cage formed with isolated ligands, and avoid the distortion of geometry of the cage, for the model E, the single-point calculation was performed to obtain the energies of each $(H_2O)_{6-n}(NH_3)_n$ cage for all metal ions. The energy components and natural bond orbital analysis were also performed by a single point calculation based on the optimized structures. The MultiWFN 3.6 program [35] was used to calculate the ITA quantities using the formatted check point file from Gaussian calculation as the input file.

3. Results and discussion

In this section, firstly, the geometric characteristics of metal ion complexes in the process of NH_3 gradually replacing H_2O have been discussed; Secondly, five types of energy calculated based on five models have been applied to quantify affinity; Thirdly, three aspects, energy decomposition analysis [21,22], NBO analysis [23] and ITA-DFRT [24] have been used to help understand the affinity.

3.1. The geometries of complexes

The most favorable coordination number of metal ions depends on the coordination environment and the nature of the ligand. For example, in the report of Rudolph et al. [36], according to Raman spectroscopy, Ca(II) is 6-coordinate in aqueous; While in the reports of Demadis et al. and Colodrero et al. [37,38], according to single crystal X-ray diffraction, both of 6-coordinate and 8-coordinate are existing. Similar phenomena have also been observed for other metal ions, such as, Sc(III) [39,40], Ti(IV) [4,41], Cu(II) [42,43], etc.. Nevertheless, the results of this work indicated that the affinity of metal ion calculated according to different coordination numbers follows the same pattern, which has been demonstrated by 6-coordinate and 8-coordinate Ca(II), Sc(III), Ti (IV) as well as 4-coordinate and 6-coordinate Cu(II) collected in Supplementary Materials. Based on this fact, only one coordination number is selected for each metal ion here.

Most of the fourteen metal ions can form 6-coordinate complexes with H_2O and/or NH_3. As reported by Varadwaj et al. [11,12], the exchange process between H_2O and NH_3 of the 6-coordinate Ni(II) complexes can be represented by ten topological structures as shown in Fig. 1. Some metal ions are not always be coordinated with six ligands. For example, Ca(II), Sc(III) and Ti(IV) can be coordinated with eight ligands, and their complexes are twisted hexahedron [4,37–41,44]; While Cu(II) can be coordinated with four ligands, and its complex is quadrilateral [42,43]. These geometric shapes are shown in Figure S1a and Figure S1b of the Supplementary Material.

As shown in Fig. 1, taking the 6-coordinate complex of Ni(II) as an example, all of the ten structures in the ligand exchange process are octahedron, which is consistent with reports in the literature [11,12]. The bond lengths of Ni-N and Ni-O are about 2.14 and 2.08 Å respectively, and the bond angles of L-Ni-L (L is NH_3 or H_2O) are about 178 ± 2 and $90 \pm 2^\circ$ respectively. For all of metal ions, the computational bond lengths of Ni-N and Ni-O agree well to the experimental result, which is $R^2 \geq 0.96$ with a small positive discrepancy (Figure S2). Additionally, as demonstrated in Fig. 1, the complexes of other metal ions coordinated with six ligands have similar shape, but the bond length and bond angle fluctuate slightly when changing the metal ions. And the exchange of H_2O with NH_3 has nothing to do with the skeleton of the complexes, the octahedron shapes are maintained during the process from $[Ni(H_2O)_6(NH_3)_0]^{2+}$ to $[Ni(H_2O)_0(NH_3)_6]^{2+}$ [11,12]. For the metal ions coordinated with eight and four ligands [44,45], the evolution of their geometry shape is similar.

3.2. Quantifying the affinity with the thermal energies calculated from different models

There are five types of energy have been usually used to describe chemical or physical process. Namely electronic energy (*E*), zero-point energy (*Z*), thermal energy (*U*), enthalpy (*H*), and Gibbs free energy (*G*) [6,46]. The electronic energy is defined by the Schrödinger equation and depends on the electron state of the molecule [21]. The other four types of energy are the eigenfunctions of the corresponding eigenstates, and are used to evaluate the spontaneity of the corresponding chemical or physical processes [47]. Herein, these five types of energy have also been used to quantify the affinity of metal ions to NH_3 and H_2O, as listed in Tables 2 and 3 with some metal ions, Mg(II), Fe(III) and Ni(II). The complete results were collected in Table S1 of Supplementary Materials.

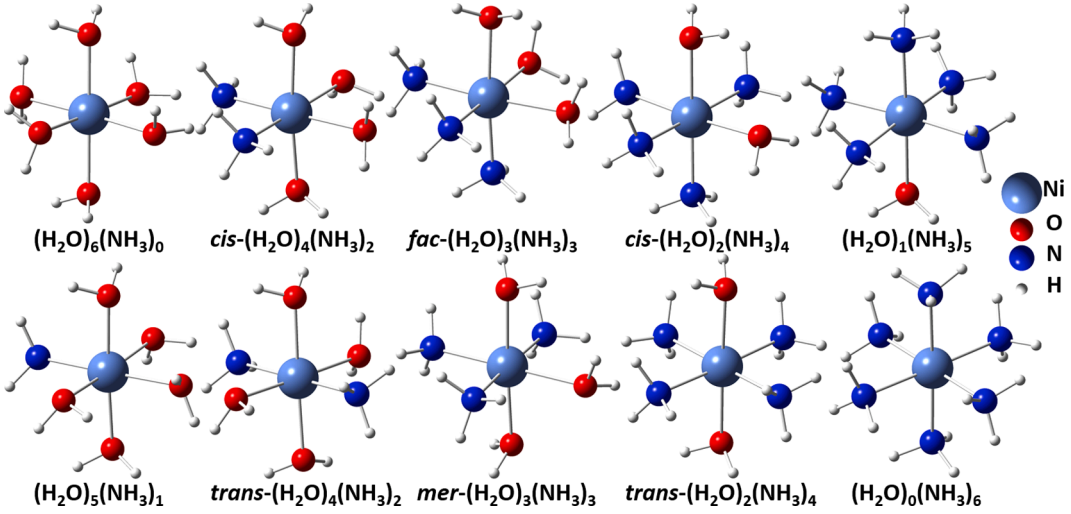

Fig. 1. The eight geometries of possible complexes in the successive ligand exchange process, using the Ni(II) as the example.

Table 2
The different thermal energies of the models A, D, and E, exampled with Mg(II), and united with kJ/mol.

Model	0*	1	*cis*_2	*trans*_2	*fac*_3	*mer*_3	*cis*_4	*trans*_4	5	6	$R^{2\#}$
A											
Δ*E*	−391	−409	−428	−428	−446	−445	−463	−463	−480	−497	
Δ*Z*	−338	−352	−371	−372	−388	−387	−407	−404	−424	−440	0.99
Δ*U*	−337	−352	−371	−371	−388	−387	−406	−404	−423	−439	0.99
Δ*H*	−352	−367	−385	−386	−403	−402	−421	−419	−438	−454	0.99
Δ*G*	−137	−145	−162	−166	−178	−173	−193	−188	−209	−223	0.98
D											
Δ*E*	0.0	−23.0	−46.4	−46.4	−69.4	−68.7	−92.0	−91.3	−114	−135	
Δ*Z*	0.0	−17.3	−39.5	−40.9	−60.3	−59.2	−82.0	−79.4	−102	−122	0.99
Δ*U*	0.0	−20.2	−43.3	−44.2	−65.6	−65.0	−88.4	−86.6	−110	−131	0.99
Δ*H*	0.0	−20.1	−43.1	−43.9	−65.2	−64.6	−87.9	−86.1	−109	−130	0.99
Δ*G*	0.0	−15.0	−39.3	−43.0	−62.0	−57.6	−84.5	−78.8	−107	−128	0.99
E											
Δ*E*	0.0	−35.2	−76.3	−73.3	−120	−117	−161	−154	−214	−260	
Δ*Z*	0.0	−29.1	−66.0	−63.0	−111	−104	−148	−142	−199	−237	0.99
Δ*U*	0.0	−24.9	−54.6	−54.3	−100	−89.9	−135	−131	−181	−218	0.99
Δ*H*	0.0	−24.9	−54.6	−54.3	−100	−89.9	−135	−131	−181	−218	0.99
Δ*G*	0.0	−34.3	−80.2	−74.9	−126	−118	−164	−154	−220	−261	0.98

* The label refers to the number of NH_3 and the configuration in the complex.
# The square of correlation coefficient with Δ*E*.

Table 3
The difference of enthalpy (Δ*H*) of five calculation models. Represented with Na(I) and Ni(II), and united with kJ/mol.

Model	0*	1	*cis*_2	*trans*_2	*fac*_3	*mer*_3	*cis*_4	*trans*_4	5	6	$R^{2\#}$
Na(I)											
A	−152	−158	−165	−165	−171	−171	−177	−177	−181	−185	
B	0.0	113	225	225	338	338	451	451	565	680	0.99
C	0.0	−5.85	−12.9	−13.2	−19.1	−19.0	−24.6	−24.6	−29.1	−33.3	1.00
D	0.0	−10.6	−22.3	−22.6	−33.2	−33.1	−43.4	−43.5	−52.6	−61.6	1.00
E	0.0	−15.1	−16.5	−14.2	−17.9	−20.7	−28.3	−29.7	−24.7	−37.5	0.87
Ni(II)											
A	−487	−530	−571	−568	−608	−605	−642	−639	−674	−704	
B	0.0	76.0	154	157	236	239	320	324	408	496	0.99
C	0.0	−42.8	−84.0	−80.5	−120	−117	−155	−152	−187	−217	1.00
D	0.0	−47.6	−93.4	−89.9	−135	−132	−174	−171	−210	−245	1.00
E	0.0	−55.8	−111	−119	−184	−179	−247	−236	−322	−384	0.99

* The label refers to the number of NH_3 and the configuration in the complex.
# The square of correlation coefficient with Δ*E*.

For different type of energy, as listed in Table 2, all types of energy have the same changing tendency during the ligand exchange process. The magnitude of energies is always increasing when the NH_3 replacing the H_2O, which is consistent with Varadwaj et al.'s reports that the NH_3 could stabilize the complexes of metal ions [11,12]. The square of correlation coefficient (R^2) between the data of Co(II) or Ni(II) calculated by us and the result reported by Varadwaj et al. is larger than 0.98 [11,12]. Additionally, in the ligand exchange process, the data listed in Tables 2 and 3 indicated that each type of energy has an approximate variate if one H_2O is replaced by one NH_3, the changing magnitude is different for different types, and the Δ*E* and Δ*G* are the largest and the smallest respectively. Moreover, all types of energy have linearly correlated each other and their R^2 are larger than 0.98. This fact indicated that every type of energy can equivalently to quantify the affinity of metal ion to ligand and to reflect its evolution in the ligand exchange process, at least in tendency.

For different models, the relative energies calculated based on different models are correlated, as demonstrated by the R^2 listed in Table 3 with the relative enthalpy (Δ*H*) of Na(I) and Ni(II). The correlation of model B, C and D could be derived from their mathematical equivalence (Table 1). However, the positive energy values of model B listed in Tables 2 and 3 indicated that its corresponding reaction equation is not a real process. Furthermore, the correlation between models A and B, C, D indicated the absolute affinity has the same tendency with relative affinity. The model E is cage exchange, namely, the metal ion moved from the cage of $(H_2O)_6$ to the cage of $(H_2O)_{6\text{-}n}(NH_3)_n$. The results of model E is still well correlated compared to other four models. This indicated that the cage-exchange model proposed in this work is also efficient to quantify the affinity of metal ions and to describe its evolution in the ligand exchange process. Comparing to other four models, the model E provide an approach to directly evaluate the affinity of metal ions to different cages, not to isolated ligands. This is practical, because metal ions in solution are usually surrounded by other molecules, most likely in a cage, rather than interacting with several isolated ligands.

Another interest phenomenon is that the stabilization energy by each NH_3 approximates to a constant, namely, during the ligand exchange process, the first NH_3 has the same stabilization contribution to the complex as well as the last NH_3 has. This was also observed by Varadwaj et al. for Ni(II) and Co(II) [11,12]. This phenomenon can be clearly demonstrated by the monotone linearly changing of the five types of relative energy, as shown in Fig. 2. Here, the Δ*E*, Δ*Z*, Δ*H*, and Δ*G* of several metal ions calculated based on model D are linearly correlated with the number of NH_3 in complex, with $R^2 > 0.95$. While, comparing to the distinguishable influence of the number of NH_3, the difference of topological configurations (*cis*- and *trans*-, *mer*- and *fac*-) have little influence on the energies. Additionally, the difference of the relative affinity of different metal ions with NH_3 and H_2O can be evaluated with the value of energies (Table 3) and directly observed from the difference of the slopes of fitted lines (Fig. 2). Moreover, according to the linear

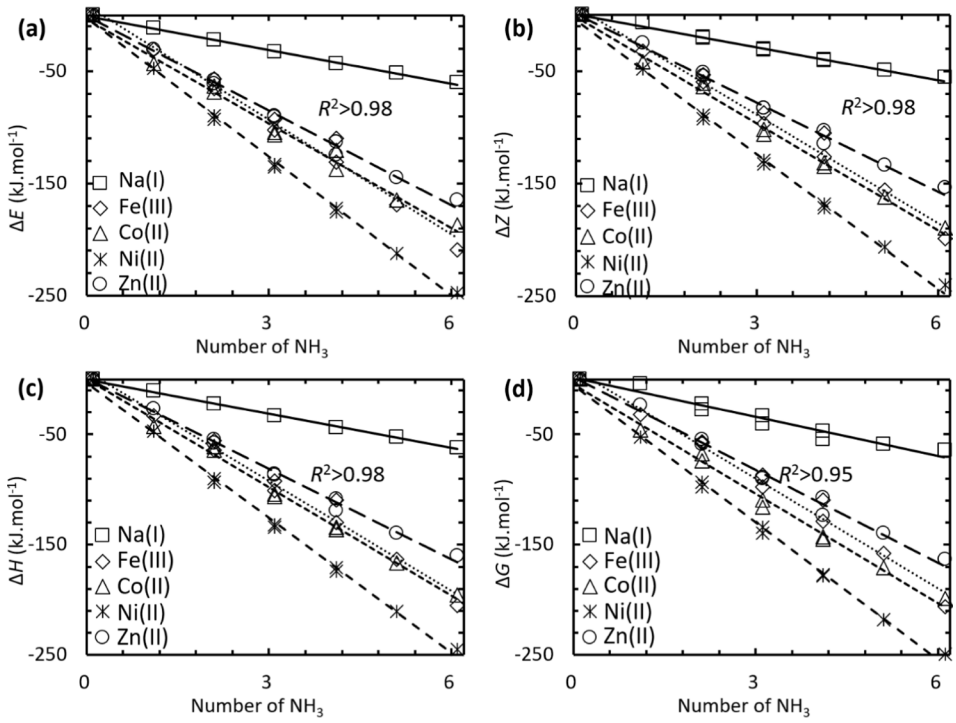

Fig. 2. The gradientally changing relative energy calculated based on model D when water was replaced with ammonia. (a), (b), (c), and (d) are refer to electronic energies, zero-point energy, enthalpy, and Gibbs Free energy respectively.

relationship between relative energy and the number of NH_3, it is can be drawn that the NH_3 or H_2O coordinated on metal ion has little influence on the ligand exchange process from the aspect of energy. It can be predicted that the difference of energies of $(H_2O)_0(NH_3)_6$ of different metal ions by those of $(H_2O)_5(NH_3)_1$, at least in tendency. Based on this principle, the first step coordination energy has been applied to estimate the total coordination energy between metal ions and acidic phosphorus-containing compounds [48].

3.3. Understanding the affinity from different aspects

As aforementioned, all of the five types of energy calculated based on the five models are available to quantify the affinity of metal ions with NH_3 and H_2O, which are consistent with Varadwaj et al.'s repots [11,12]. However, the reports about the understanding of the affinity are rare [9]. Herein, we attempt to provide the understanding of affinity from three aspects, energy decomposition analysis [21,22], natural bond orbital analysis [23] and information-theoretic approach in density functional reactivity theory [24]. Some representative quantities calculated based on these three aspects are listed in Table 4 with the Ni (II) as the example, the correlation coefficients between these quantities and the relative affinity quantified with relative Gibbs free energy (ΔG) are collected in Table 5, and some cases are plotted in Fig. 3.

3.3.1. With energy decomposition analysis

The ΔE_e, ΔT_s, and ΔE_{XC} of ligand exchange process of Ni(II) were listed in Table 4. Their magnitude illustrated that the E_e and T_s provide the main positive and negative contribution to the total energy changing during the ligand exchange process, although the contribution of E_{XC} is very small. According to their large correlation coefficients (Table 5)

Table 4
Some quantities of mixture complex, using the Ni(II) as an example. The *trans*_2, *mer*_3, and *trans*_4 is not presented due to the limitation of width. The relative values are calculated based on model D. The quantities from natural bond orbital analysis and absolute ITA quantities belong to the central metal ions, but the relative ITA quantities belong to the whole molecule.

Quantities	0*	1	*cis*_2	*fac*_3	*cis*_4	5	6
ΔE_e	0.00	−444444	−888872	−1333302	−1777714	−2222097	−2666474
ΔT_s	0.00	163,583	327,151	490,724	654,282	817,814	981,341
ΔE_{XC}	0.00	−37.16	−70.54	−104.17	−132.97	−157.81	−183.55
ESP	1.6415	1.5188	1.6619	1.6333	1.6623	1.5895	1.6896
Hirshfeld	0.49456	0.48257	0.47201	0.46231	0.45589	0.45284	0.45104
NPA	1.1251	1.0606	0.9988	0.9402	0.8833	0.8324	0.7774
MEP	−128.257	−128.280	−128.300	−128.321	−128.337	−128.351	−128.364
NAO_all	8.85005	8.91440	8.97540	9.03266	9.08795	9.13689	9.18894
I_F	6109.476	6109.035	6108.571	6108.159	6107.714	6107.534	6107.180
E_2	5114.533	5114.645	5114.731	5114.800	5114.871	5114.913	5114.920
$^rR_2$	27.1166	27.1565	27.2088	27.2864	27.2587	27.3535	27.3509
ΔI_F	0.00	−0.6197	−1.1781	−1.7149	−2.2081	−2.6272	−3.1417
ΔE_2	0.00	−0.0538	−0.0988	−0.0041	−0.0003	−0.0366	−0.0150
Δ^rR_2	0.00	0.1268	0.2292	0.3139	0.4084	0.4624	0.4871

* The number of NH_3 in complex.

Table 5
The correlation coefficients between ΔG and other quantities.

Quantities	Na(I)	Mg(II)	Al(III)	Sc(III)	V(II)	Mn(II)	Fe(III)	Co(II)	Ni(II)	Zn(II)
ΔE_e	0.977	0.997	0.999	0.997	0.998	0.996	0.991	0.996	**0.998**	0.995
ΔT_s	−0.977	−0.997	−0.999	−0.997	−0.998	−0.996	−0.991	−0.996	**−0.998**	−0.995
ΔE_{XC}	0.976	0.995	0.917	0.990	0.990	0.979	0.979	0.979	**0.999**	0.950
ESP	0.758	−0.605	−0.236	0.491	0.840	0.981	0.596	0.816	−0.204	0.731
Hirshfeld	−0.969	−0.549	0.990	0.974	0.930	0.989	0.976	0.976	0.971	0.897
NPA	0.952	0.989	0.999	0.982	0.985	0.994	0.988	0.993	**0.998**	0.952
MEP	0.977	0.997	0.999	0.994	0.996	0.991	0.987	0.996	0.999	0.987
NAO_all	−0.977	−0.997	−0.999	−0.992	−0.996	−0.991	−0.988	−0.996	**−0.999**	−0.989
I_F	0.970	0.989	0.999	0.988	0.992	0.997	0.991	0.985	**0.993**	0.994
E_2	0.706	−0.944	−0.949	0.957	−0.993	−0.994	−0.939	−0.953	**−0.965**	−0.905
$^rR_2$	−0.481	−0.826	−0.897	−0.981	−0.405	−0.977	−0.977	−0.933	−0.892	−0.948
ΔI_F	0.961	0.990	−0.915	0.983	0.990	0.986	0.968	0.982	**0.998**	0.960
ΔE_2	0.023	−0.528	−0.910	−0.713	0.249	−0.634	−0.806	0.052	−0.157	−0.640
Δ^rR_2	−0.975	−0.993	−0.986	−0.727	−0.997	−0.996	−0.956	−0.968	**−0.979**	−0.919

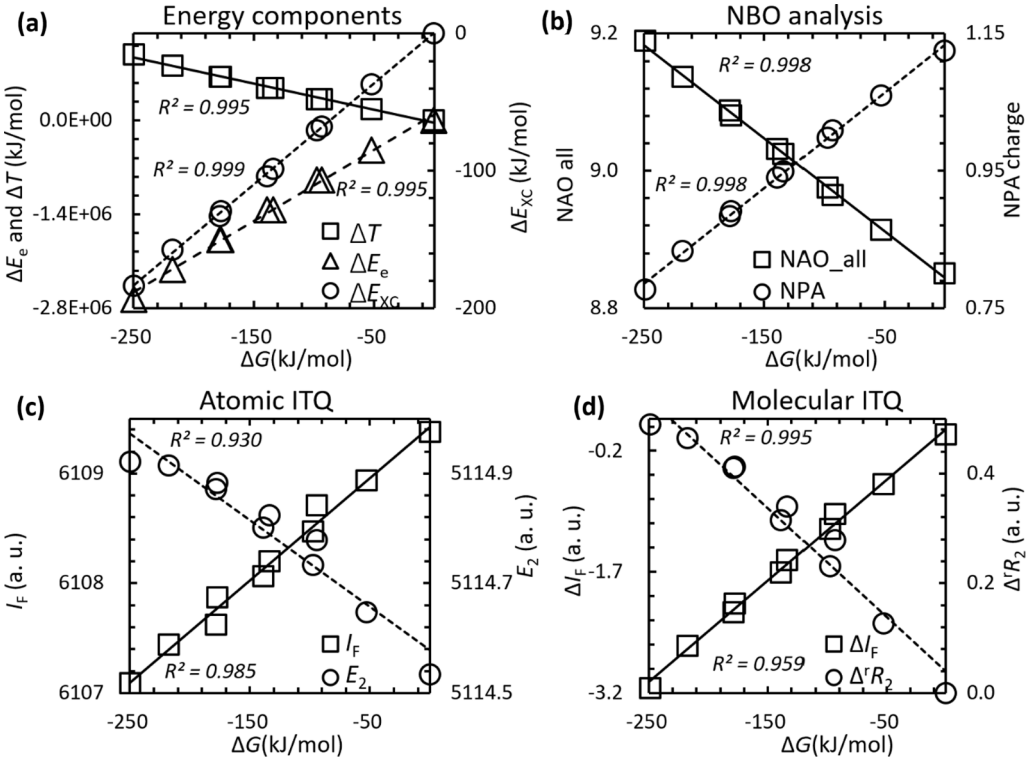

Fig. 3. The linear relationship between relative Gibbs free energies and other quantities, using the ΔG of Ni(II) calculated from model D as the examples (bold marked cells in Table 5). (a) The energy components, (b) the MEP and NAO_all (summary of occupation number of valence s, p, and 4 orbital), (c) the ITQ of central metal, and (d) the relative ITQ calculated as model D of whole molecule.

and definite linear relationship (Fig. 4(a)), these three components are necessary to the total energy. And these facts suggest that the relative affinity of metal ions can be understood by the energy components. In DFT, the energy is conventionally decomposed to three components, E_e, T_s and E_{XC}. E_e is the electronic energy, which represents classical coulombic interaction energy [22]. NH_3 could provide larger electron density than H_2O at the bond crucial points [11], resulting in stronger E_e. Therefore, the E_e is positively correlated to the number of NH_3, and positively correlated to the ΔG. In fact, the E_e is closely related to the atomic hardness and softness [22]. The interaction between metal ion and ligand could be described well by the HSAB [18]. It is predictable that E_e should also be able to describe the affinity. For the other two quantities, T_s is another major component [21], and its contribution to the total energy is opposite to E_e. Therefore, it has a negative correlation with ΔG. E_{XC} is a little component in whole energy, and its correlation was mostly depended on exchange energy. The exchange energy is non-classic electrostatic interaction of electron [21], which is similar to the E_e and has positive correlation to the ΔG.

3.3.2. With NBO quantities

Several representative quantities of NBO analysis, including atomic charge (ESP, Hirshfeld and NPA), molecular electrostatic potential (MEP) and population of natural atomic valence orbital of central metal ions (NAO_all is presented here, and other NAO quantities are collected in Table S2), were collected in Table 4. Their correlation coefficients with affinity (ΔG) were collected in Table 5. For the atomic charge, the ESP charge is not monotonic changing with the number of NH_3, and has a small correlation coefficient (Table 5). Therefore, the ESP charge is not suitable to comprehend the affinity. While, both of Hirshfeld and NPA charges show a rigorous monotonous changing, as demonstrated with

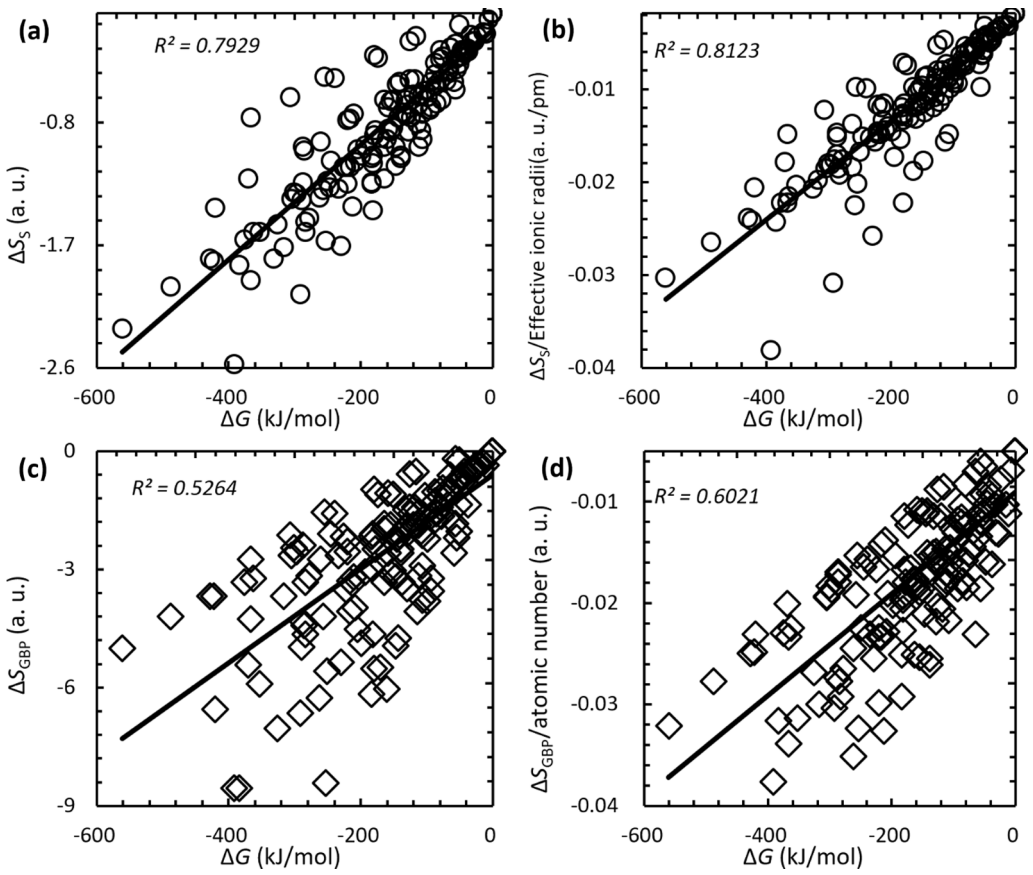

Fig. 4. The relationship between relative Gibbs free energies and relative ITQ fitting together. The (a) and (c) refer to the original relative Shannon entropy and GBP entropy, and the (b) and (d) refer to modified Shannon entropy and GBP entropy with effective ionic radii and atomic number.

the large and negative correlation coefficients in Table 5. The lower charge values on the metal ion correspond to the larger number of NH_3, which is consistent with Varadwaj et al.'s reports that the NH_3 is favorable to charge transferring from ligand to metal ions [11,12]. The MEP and NAO from NBO analysis also present special changing rules. The three quantities of NPA charge, MEP and NAO are intrinsically related to the atomic charge, especial the NPA charge. It is positively and negatively correlated to the MEP and NAO respectively [23]. Consequently, these quantities from NBO analysis are suitable to understand the affinity except the ESP charge.

3.3.3. *With ITA quantities*

Two types of ITA quantities, which are belonging to metal ions and whole molecules respectively, are collected in Table 4. Their correlation coefficients with ΔG based on model D are collected in Table 5. The difference of absolute ITA quantities mainly contributed from the changings of the number and/or type of atoms in complexes [24]. It should be noted that the ITA quantities of the whole molecule are relative value by calculating based on model D, as the absolute value could not be compared directly. It is shown that the atomic ITA quantities of central metal ions are distinct monotonous increasing or decreasing as the changings of the number of NH_3 (Table 4, S3a). The correlation coefficients of atomic ITA quantities with ΔG (Table 5) are mostly good to excellent, and the plotting of linear relationship are also shown in Fig. 3(c). For the molecular ITA quantities, as the correlation coefficients (Table 5) and the fitting lines (Fig. 3(d)) illustrated, most cases (ΔS_S, ΔI_F, ΔS_{GBP}, $\Delta^r R_2$, etc.) are monotonous fluctuation as the changings of the numbers of NH_3. However, the ΔI_G and ΔE_2 are not monotonous fluctuation. These facts distinguish if the atomic and molecular ITA quantities was valid to understand the affinity from the aspect of distribution of electron density.

As aforementioned, all the energy components, some quantities from NBO analysis, and ITA quantities have good to excellent linear correlation with affinity as fitting by individual metal ion. However, these quantities are difficult to directly compare the affinity with different metal ions. To provide a uniform measurement for the affinity, we have tried to fit all metal ions together. We supposed that if the uniform measurement was existing, all metal ions could be fitted into the same line. Therefore, the shared fitted trendline and its R^2 are applied to quantify the collinearity of all plots. However, both of the energy components and the energy quantities from NBO analysis are not fitting efficiently, while some ITA quantities have medium feasibility. As shown in Fig. 4(a) and (c), taking the relative Shannon entropy (ΔS_S) and GBP entropy (ΔS_{GBP}) as the examples, their R^2 are 0.7929 and 0.5264 respectively. Therefore, both of which are not satisfactory results. The points could be obviously fitted into several trendlines with different slopes in both of Fig. 4(a) and (c), with each line represents the corresponding metal ion. To improve the fitting results, various modification approaches using different intrinsic properties of ions have been attempted, and the slightly better fitting results were obtained and presented in Fig. 4(b) and (d). The effective ionic radii and atomic number of central metal ions have been applied [49], with their R^2 are 0.8123 and 0.6021 respectively. The Fig. 4 indicates that ITA-DFRT is a potential tool to build the uniform measurement to the affinity of different metal ions.

4. Conclusion

In this work, at first, the affinity between fourteen metal ions with the NH_3 and/or H_2O were studied. Five types of energy calculated based on five ligand-exchange models were regarded as the measurement of the affinity. The results indicated that the novel cage-exchange model

proposed by us is effective as well as the other four models in quantifying the affinity between metal ions and ligands. Secondly, the correlation analysis demonstrated that the three approaches, energy decomposition analysis, NBO analysis and ITA-DFRT are useful to understand the affinity from the aspects of energy components, NBO quantities, and electron density distribution characteristic respectively. Thirdly, the ITA-DFRT has been found potential to build a uniform system in measuring the affinity of different metal ions.

CRediT authorship contribution statement

Xue-Yun Shang: Data curation, Formal analysis, Writing - original draft. **Hua-Ying An:** Investigation, Methodology, Project administration, Resources. **Ting Zhang:** Data curation, Investigation, Methodology, Resources. **Jin-Hong Lin:** Methodology, Project administration. **Fei Hao:** Writing - review & editing. **Dong-Hai Yu:** Investigation, Visualization. **Ji-Chang Xiao:** Supervision, Funding acquisition. **Tian-Duo Li:** Supervision, Funding acquisition.

Declaration of Competing Interest

The authors declare that they have no known competing financial interests or personal relationships that could have appeared to influence the work reported in this paper.

Acknowledgments

This work was supported by the financial support from Program for Scientific Research Innovation Team in Colleges and Universities of Shandong Province, and Jinan Science and Technology Bureau (2019GXRC021), the National Natural Science Foundation (21421002, 21672242, 21971252, 21991122), Key Research Program of Frontier Sciences (CAS) (QYZDJSSW-SLH049), Youth Innovation Promotion Association CAS (2019256), the Fujian Institute of Innovation, Chinese Academy of Sciences (FJCXY18040102). Computing resources were provided by the National Supercomputing Center of China in Shenzhen.

Appendix A. Supplementary material

Supplementary data to this article can be found online at https://doi.org/10.1016/j.cplett.2021.138398.

References

[1] R.C.F. Cheung, J.H. Wong, T.B. Ng, Appl. Microbiol. Biotechnol. 96 (2012) 1411.
[2] M.L. Renart, E. Montoya, A.M. Fernández, M.L. Molina, J.A. Poveda, J.A. Encinar, J.L. Ayala, A.V. Ferrer-Montiel, J. Gómez, A. Morales, J.M. González Ros, Biochemistry-us 51 (2012) 3891.
[3] K.I. Assaf, W.M. Nau, Chem. Soc. Rev. 44 (2015) 394.
[4] J. van Sijl, N.L. Allan, G.R. Davies, W. van Westrenen, Phys. Chem. Chem. Phys. 13 (2011) 7371.
[5] J. Jover, R. Bosque, J. Sales, Dalton Trans. 37 (2008) 6441.
[6] T. Marino, N. Russo, M. Toscano, J. Phys. Chem. B 107 (2003) 2588.
[7] G.D. Markham, J.P. Glusker, C.L. Bock, M. Trachtman, C.W. Bock, J. Phys. Chem. 100 (1996) 3488.
[8] B. Kallies, R. Meier, Inorg. Chem. 40 (2001) 3101.
[9] A.N. Kucharski, C.E. Scott, J.P. Davis, P.M. Kekenes-Huskey, J. Phys. Chem. B 120 (2016) 8617.
[10] K.-F. Mo, Z. Dai, D.S. Wunschel, J. Nat. Prod. 79 (2016) 1492.
[11] P.R. Varadwaj, I. Cukrowski, H.M. Marques, J. Phys. Chem. A 112 (2008) 10657.
[12] P.R. Varadwaj, H.M. Marques, Phys. Chem. Chem. Phys. 12 (2010) 2126.
[13] P.R. Varadwaj, H.M. Marques, Theor. Chem. Acc. 127 (2010) 711.
[14] H.H. Tam, D. Asthagiri, M.E. Paulaitis, J. Chem. Phys. 137 (2012), 164504.
[15] N. Dehghani, B. Ghalami-Choobar, M. Arabieh, H. Dezhampanah, Struct. Chem. 30 (2019) 1437.
[16] H. Chen, R. Shi, H. Ow, ACS Omega 4 (2019) 20665.
[17] P.R. Varadwaj, A. Varadwaj, B.-Y. Jin, Phys. Chem. Chem. Phys. 17 (2015) 805.
[18] R.D. Hancock, A.E. Martell, Chem. Rev. 89 (1989) 1875.
[19] P. D'Angelo, V. Barone, G. Chillemi, N. Sanna, W. Meyer-Klaucke, N.V. Pavel, J. Am. Chem. Soc. 124 (2002) 1958.
[20] P.R. Varadwaj, I. Cukrowski, C.B. Perry, H.M. Marques, J. Phys. Chem. A 115 (2011) 6629.
[21] R.G. Parr, W.T. Yang, Density-functional theory of atoms and molecules, Oxford University Press, Madison Avenue, New York, 10016, 1989.
[22] P. Geerlings, F.D. Proft, W. Langenaeker, Chem. Rev. 103 (2003) 1793.
[23] E.D. Glendening, C.R. Landis, F. Weinhold, WIREs: Comput. Mol. Sci. 2 (2012) 1.
[24] C.Y. Rong, B. Wang, D.B. Zhao, S.B. Liu, WIREs: Comput. Mol. Sci. 10 (2020), e1461.
[25] H.M. Lee, S.B. Suh, J.Y. Lee, P. Tarakeshwar, K.S. Kim, J. Chem. Phys. 112 (2000) 9759.
[26] H. Nakai, T. Goto, T. Ichikawa, Y. Okada, T. Orii, K. Takeuchi, Chem. Phys. 262 (2000) 201.
[27] R. Ludwig, Angew. Chem. Int. Ed. 40 (2001) 1808.
[28] S.B. Liu, J. Phys. Chem. A 117 (2013) 962.
[29] D.H. Yu, C.Y. Rong, T. Lu, P. Geerlings, F. De Proft, M. Alonso, S.B. Liu, Phys. Chem. Chem. Phys. 22 (2020) 4715.
[30] R.O. Esquivel, S.B. Liu, J.C. Angulo, J.S. Dehesa, J. Antolín, M. Molina-Espíritu, J. Phys. Chem. A 115 (2011) 4406.
[31] S.B. Liu, C.Y. Rong, T. Lu, J. Phys. Chem. A 118 (2014) 3698.
[32] Y. Zhao, D.G. Truhlar, Theor. Chem. Acc. 120 (2008) 215.
[33] V.A. Rassolov, M.A. Ratner, J.A. Pople, P.C. Redfern, L.A. Curtiss, J. Comput. Chem. 22 (2001) 976.
[34] G.W.T. M. J. Frisch, H. B. Schlegel, G. E. Scuseria, M. A. Robb, J. R. Cheeseman, G. Scalmani, V. Barone, B. Mennucci, G. A. Petersson, H. Nakatsuji, M. Caricato, X. Li, H. P. Hratchian, A. F. Izmaylov, J. Bloino, G. Zheng, J. L. Sonnenberg, M. Hada, M. Ehara, K. Toyota, R. Fukuda, J. Hasegawa, M. Ishida, T. Nakajima, Y. Honda, O. Kitao, H. Nakai, T. Vreven, J. A. Montgomery, Jr., J. E. Peralta, F. Ogliaro, M. Bearpark, J. J. Heyd, E. Brothers, K. N. Kudin, V. N. Staroverov, T. Keith, R. Kobayashi, J. Normand, K. Raghavachari, A. Rendell, J. C. Burant, S. S. Iyengar, J. Tomasi, M. Cossi, N. Rega, J. M. Millam, M. Klene, J. E. Knox, J. B. Cross, V. Bakken, C. Adamo, J. Jaramillo, R. Gomperts, R. E. Stratmann, O. Yazyev, A. J. Austin, R. Cammi, C. Pomelli, J. W. Ochterski, R. L. Martin, K. Morokuma, V. G. Zakrzewski, G. A. Voth, P. Salvador, J. J. Dannenberg, S. Dapprich, A. D. Daniels, O. Farkas, J. B. Foresman, J. V. Ortiz, J. Cioslowski, D. J. Fox, Gaussian 09, Revision D. 01, Gaussian, Inc., Wallingford, CT. Gaussian, Inc. Wallingford, CT, 2013.
[35] T. Lu, F.W. Chen, J. Comput. Chem. 33 (2012) 580.
[36] W.W. Rudolph, G. Irmer, Dalton Trans. 42 (2013) 3919.
[37] R.M.P. Colodrero, A. Cabeza, P. Olivera-Pastor, M. Papadaki, J. Rius, D. Choquesillo-Lazarte, J.M. García-Ruiz, K.D. Demadis, M.A.G. Aranda, Cryst. Growth Des. 11 (2011) 1713.
[38] K.D. Demadis, M. Papadaki, I. Císařová, ACS Appl. Mater. Interfaces 2 (2010) 1814.
[39] S.A. Cotton, Comments Inorg. Chem. 21 (1999) 165.
[40] A. Abbasi, P. Lindqvist-Reis, L. Eriksson, D. Sandström, S. Lidin, I. Persson, M. Sandström, Chem.-Eur. J. 11 (2005) 4065.
[41] M.-H. Xie, X.-L. Yang, Y. He, J. Zhang, B. Chen, C.-D. Wu, Chem.-Eur. J. 19 (2013) 14316.
[42] M. Valli, S. Matsuo, H. Wakita, T. Yamaguchi, M. Nomura, Inorg. Chem. 35 (1996) 5642.
[43] L. Wang, L. Duan, D. Xiao, E. Wang, C. Hu, J. Coord. Chem. 57 (2004) 1079.
[44] A. Mishra, W. Wernsdorfer, K.A. Abboud, G. Christou, Chem. Commun. (2005) 54.
[45] S.V.F. Beddoe, R.F. Lonergan, M.B. Pitak, J.R. Price, S.J. Coles, J.A. Kitchen, T. D. Keene, Dalton Trans. 48 (2019) 15553.
[46] J.A. Hebda, Z. Aamold, J. Chem. Educ. 96 (2019) 1686.
[47] E. Fermi, Thermodynamics, Dover Publications, New York, 1956.
[48] Y.-Q. Xiang, X. Yao, J.-H. Lin, X.-J. Ou, R. Li, Y.-S. Zhou, D.-H. Yu, J.-C. Xiao, J. Phys. Chem. A 124 (2020) 5033.
[49] J.Y. Wu, D.H. Yu, S.Y. Liu, C.Y. Rong, A.G. Zhong, P.K. Chattaraj, S.B. Liu, J. Phys. Chem. A 123 (2019) 6751.